

## ENDOR Determination of the Distance between Bleomycin-Bound Iron and $^{19}\text{F}$ of 2'-Fluorocytidine in a DNA Target Sequence

Dmitriy Lukoyanov,<sup>§,†</sup> Richard M. Burger,<sup>#,§</sup> and Charles P. Scholes<sup>\*,§</sup>

Department of Chemistry and Center for Biological Macromolecules, State University of New York at Albany  
Albany, New York 12222  
Public Health Research Institute, 455 First Avenue  
New York, New York 10016

Received August 26, 2001

In the presence of Fe(II),  $\text{O}_2$ , and reductant, activated bleomycin (Act-BLM) transiently arises as the kinetically competent form leading to DNA cleavage. Act-BLM and its final product, ferric bleomycin (Fe(III)-BLM), are low-spin ferric complexes.<sup>1,2b</sup> Act-BLM has  $g_{\text{max}}$ ,  $g_{\text{inter}}$ ,  $g_{\text{min}}$  = 2.26, 2.17, 1.94, and Fe(III)-BLM has  $g_{\text{max}}$ ,  $g_{\text{inter}}$ ,  $g_{\text{min}}$  = 2.45, 2.18, 1.89.<sup>2</sup> Understanding bleomycin action<sup>3</sup> requires knowing the physical and electronic nature of the BLM–oligonucleotide complexes. NMR-derived structures were first determined from nonparamagnetic, nonactive Zn-BLM<sup>4a,b</sup> and CO-Fe(II)-BLM forms.<sup>4c</sup> Next, NMR structures of stable, nonparamagnetic HOO-Co(III)-BLM–oligonucleotide complexes showed proximity of the hydrogen on the hydroperoxy HOO<sup>-</sup> metal ligand to the sugar H4'.<sup>5</sup> With iron-containing Act-BLM, a spontaneous oxidative attack abstracts this H4'.<sup>6</sup>

Fe(III)-BLM and Act-BLM have not been crystallized, either by themselves or as oligonucleotide complexes. Furthermore, these Fe(III)-containing forms are not amenable to structural NMR because the ferric ion is a strong relaxer and Act-BLM is unstable in solution. However, electron nuclear double resonance (ENDOR) can reveal structural and electronic information on these paramagnetic Fe(III) forms. ENDOR has resolved nearest-neighbor hyperfine structure from nitrogen ligands, from axial exchangeable H, and, for Act-BLM, from the bound hydro-

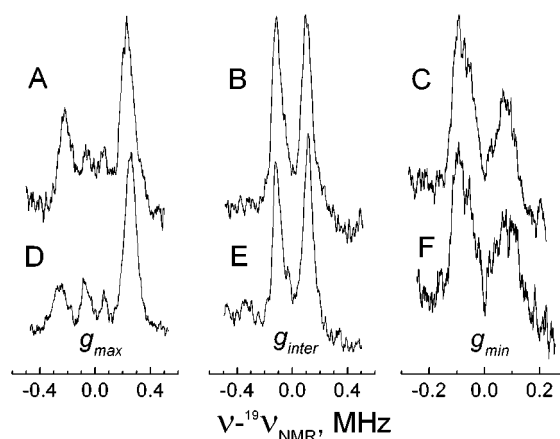


**Figure 1.**  $^{19}\text{F}$  ENDOR spectra centered at the appropriate  $^{19}\text{V}_{\text{NMR}}$  were obtained under adiabatic rapid passage conditions with small ( $\sim 0.12$  G) 100 kHz field modulation,  $\sim 0.25$   $\mu\text{W}$  microwave power, and  $\sim 20$  W radio frequency power, in a sweep time of 5 s. Each spectrum for Act-BLM was compiled in  $\sim 30$  min, and each Fe(III)-BLM spectrum was collected in  $\sim 1$  h. Spectra A–C from Act-BLM were (A) at  $g = 2.26$ ,  $H = 1.08$  T; (B) at  $g = 2.17$ ,  $H = 1.12$  T; (C) at  $g = 1.94$ ,  $H = 1.26$  T. Spectra D–F from Fe(III)-BLM were (D) at  $g = 2.43$ ,  $H = 1.00$  T; (E) at  $g = 2.18$ ,  $H = 1.12$  T; (F) at  $g = 1.89$ ,  $H = 1.29$  T.

peroxide derived from  $^{17}\text{O}_2$ .<sup>7a</sup> ENDOR has demonstrated bleomycin interaction with a DNA 10-mer duplex, d(GGAAGCTTCC)<sub>2</sub>, containing a 5'-G-pyr-3' sequence favored for DNA cleavage.<sup>7b</sup> DNA  $^{31}\text{P}$ -to-Fe(III) dipolar couplings indicated an Fe(III)-to- $^{31}\text{P}$  phosphate (unassigned<sup>7b</sup>) distance of 7.4 Å.<sup>8</sup>

Our aim is now to measure the distance and orientation from Fe(III) in both Act-BLM and Fe(III)-BLM to the target cytidine sugar in the 5'-G-C-3' sequence. To pinpoint this cytidine, this sugar was labeled with ENDOR-detectable  $^{19}\text{F}$  replacing H2'' at its 2' carbon; thus, the oligonucleotide d(GGAAGC<sup>F</sup>TTCC)<sub>2</sub> was used, where C<sup>F</sup> is 2'-F-cytidine.<sup>9</sup> Samples of Fe(III)-BLM and Act-BLM in deuterated solvent and in a slight molar excesses of (GGAAGC<sup>F</sup>TTCC)<sub>2</sub> were prepared as described previously for d(GGAAGCTTCC)<sub>2</sub><sup>7b</sup> (see Supporting Information). Samples ( $\sim 50$   $\mu\text{L}$ ) contained 0.6 mM Act-BLM or 1.4 mM Fe(III)-BLM. The respective  $g$ -values of Fe(III)-BLM and Act-BLM were unchanged by these oligonucleotides. The Q-band spectrometer<sup>10</sup> and conditions<sup>7b</sup> were as previously described.

The hyperfine-coupled spin  $1/2$  nucleus of  $^{19}\text{F}$  has first-order ENDOR frequencies,  $^{19}\text{V}_{\text{ENDOR}} = |^{19}\text{V}_{\text{NMR}} \pm A/2|$ , where  $^{19}\text{V}_{\text{NMR}}$  is the  $^{19}\text{F}$  NMR frequency (48.06 MHz at 1.200 T) and  $A$  is the hyperfine coupling. Figure 1 shows  $^{19}\text{F}$  ENDOR spectra centered at  $^{19}\text{V}_{\text{NMR}}$  for the d(GGAAGC<sup>F</sup>TTCC)<sub>2</sub> complexes with Act-BLM (spectra A–C) or Fe(III)-BLM (spectra D–F) near their respective  $g_{\text{max}}$ ,  $g_{\text{inter}}$ , and  $g_{\text{min}}$ .  $^{19}\text{F}$  provided distinctly anisotropic ENDOR splittings. For Act-BLM and Fe(III)-BLM, respectively, the hyperfine splittings, measured as splittings between maxima of the ENDOR spectra, were as follows: at  $g_{\text{max}}$ ,  $0.45 \pm 0.01$  and

(7) (a) Veselov, A.; Sun, H.; Sienkiewicz, A.; Taylor, H.; Burger, R. M.; Scholes, C. P. *J. Am. Chem. Soc.* **1995**, *117*, 7508–7512. (b) Veselov, A.; Burger, R. M.; Scholes, C. P. *J. Am. Chem. Soc.* **1998**, *120*, 1030–1033.

(8) NOESY cross peaks used in constraining interproton distances define shorter distances than those that ENDOR can define between paramagnetic metal centers and  $^{19}\text{F}$  or  $^{31}\text{P}$ .

(9) d(GGAAGC<sup>F</sup>TTCC), containing C<sup>F</sup> as 2'-F-cytidine and all other sugars in their deoxy form, was purchased from Trilink Biotechnologies (San Diego, CA) with double HPLC purification. The melting temperature of d(GGAAGC<sup>F</sup>TTCC)<sub>2</sub> and d(GGAAGCTTCC)<sub>2</sub> was 32 °C, determined spectrophotometrically. Prior to preparation of BLM–oligonucleotide complexes, 20 mM d(GGAAGC<sup>F</sup>TTCC) was dissolved in 20 mM pH 7.8 deuterated buffer, heated to 75 °C, and slowly chilled over 1 h to provide 10 mM d(GGAAGC<sup>F</sup>TTCC)<sub>2</sub>.

(10) Sienkiewicz, A.; Smith, B. G.; Veselov, A.; Scholes, C. P. *Rev. Sci. Instrum.* **1996**, *67*, 2134–2138.

\* To whom correspondence should be addressed.

<sup>§</sup> SUNY at Albany.

<sup>#</sup> Public Health Research Institute.

<sup>†</sup> On leave from the MRS Laboratory, Kazan State University, 420008, Kazan, Russian Federation.

(1) Kuramochi, H.; Takahashi, K.; Takita, T.; Umezawa, H. *J. Antibiot.* **1981**, *34*, 576–582.

(2) (a) Burger, R. M.; Peisach, J.; Blumberg, W. E.; Horwitz, S. B. *J. Biol. Chem.* **1979**, *254*, 10906–10912. (b) Burger, R. M.; Peisach, J.; Horwitz, S. B. *J. Biol. Chem.* **1981**, *256*, 11636–11644.

(3) (a) Stubbe, J.; Kozarich, J. W.; Wu, W.; Vanderwall, D. E. *Acc. Chem. Res.* **1996**, *29*, 322–330. (b) Stubbe, J.; Kozarich, J. W. *Chem. Rev.* **1987**, *87*, 1107–1136. (c) Burger, R. M. *Chem. Rev.* **1998**, *98*, 1153–1169. (d) Solomon, E. I.; Brunold, T. C.; Davis, M. I.; Kemsley, J. N.; Lee, S.-K.; Lehnert, N.; Neese, F.; Skulan, A. J.; Yang, Y.-S.; Zhou, J. *Chem. Rev.* **2000**, *100*, 235–349.

(4) (a) Manderville, R. A.; Ellena, J. F.; Hecht, S. M. *J. Am. Chem. Soc.* **1995**, *117*, 7891–7903. (b) Manderville, R. A.; Ellena, J. F.; Hecht, S. M. *J. Am. Chem. Soc.* **1994**, *116*, 10851–10852. (c) Akkerman, M. A. J.; Neijman, E. W. J. F.; Wijmenga, S. S.; Hilbers, C. S.; Bermel, W. *J. Am. Chem. Soc.* **1990**, *112*, 7462–7474.

(5) (a) Wu, W.; Vanderwall, D. E.; Turner, C. J.; Kozarich, J. W.; Stubbe, J. *J. Am. Chem. Soc.* **1996**, *118*, 1281–1294. (b) Mao, Q.; Fulmer, P.; Li, W.; DeRose, E. F.; Petering, D. H. *J. Biol. Chem.* **1996**, *271*, 6185–6191. (c) Vanderwall, D. E.; Lui, S. M.; Wu, W.; Turner, C. J.; Kozarich, J. W.; Stubbe, J. *Chem. Biol.* **1997**, *4*, 373–387. (d) Fulmer, P.; Zhao, C.; Li, W.; DeRose, E.; Antholine, W. E.; Petering, D. H. *Biochemistry* **1997**, *36*, 4367–4374. (e) Caceres-Cortes, J.; Sugiyama, H.; Ikudome, K.; Saito, I.; Wang, A. H. *Biochemistry* **1997**, *36*, 9995–10005. (f) Wu, W.; Vanderwall, D. E.; Teramoto, S.; Lui, S. M.; Hoehn, S.; Tang, X.-J.; Turner, C. J.; Boger, D. L.; Kozarich, J. W.; Stubbe, J. *J. Am. Chem. Soc.* **1998**, *120*, 2239–2250. (g) Hoehn, S. T.; Junker, H. D.; Bunt, R. C.; Turner, C. J.; Stubbe, J. *Biochemistry* **2001**, *40*, 5894–5905.

(6) Wu, J. C.; Kozarich, J. W.; Stubbe, J. *Biochemistry* **1985**, *24*, 7562–7568.

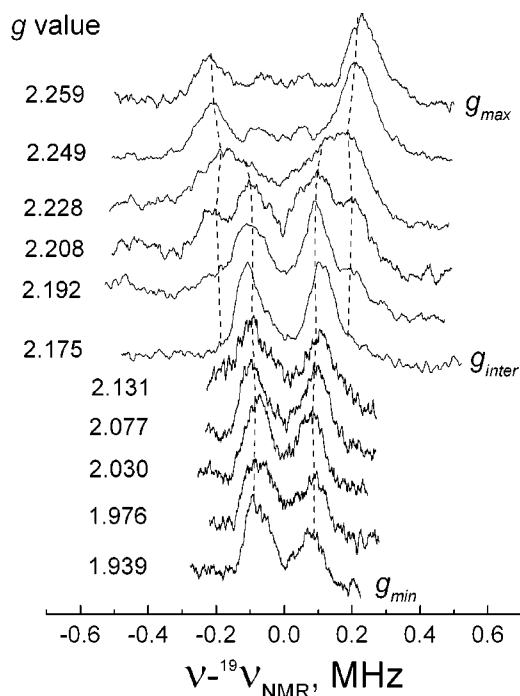


**Figure 2.** The  $g$  value dependence of  $^{19}\text{F}$  ENDOR features from Act-BLM with  $\text{d}(\text{GGAAGC}^{\text{FTTCC}})_2$ . The experimental conditions were as for Figure 1. The dashed lines show the values predicted for outlying splittings modeled from an anisotropic hyperfine tensor having  $A_z, A_y, A_x = 0.48, -0.23, -0.20$  MHz and the  $\text{Fe}(\text{III})\text{-}^{19}\text{F}$  vector ( $\mathbf{R}$ ) pointing at  $10^\circ$  to the  $g_{\text{max}}$  axis in the  $g_{\text{max}}\text{-}g_{\text{min}}$  plane. The signal-to-noise was approximately 2-fold better in the  $g_{\text{max}}\text{-}g_{\text{inter}}$  region, where the underlying EPR signal is larger. In the  $g_{\text{inter}}\text{-}g_{\text{min}}$  region there were no  $^{19}\text{F}$  splittings greater than 0.5 MHz.

$0.51 \pm 0.02$  MHz; at  $g_{\text{inter}}$ ,  $0.21 \pm 0.01$  MHz and  $0.23 \pm 0.01$  MHz; at  $g_{\text{min}}$ ,  $0.16 \pm 0.03$  and  $0.16 \pm 0.03$  MHz. There was also a smaller  $^{19}\text{F}$  splitting of about  $0.13 \pm 0.02$  MHz observed only near  $g_{\text{max}}$ . Figure 2 shows the systematic shift of  $^{19}\text{F}$  ENDOR frequencies of Act-BLM features as the  $g$ -value varied from  $g_{\text{max}}$  to  $g_{\text{min}}$ . The experimentally most distinct ENDOR features were the outlying features, with frequencies readily computable by angle-selected ENDOR theory<sup>11</sup> (dashed lines, Figure 2). The input parameters for angle-selected computations that predict outlying features were the principal elements of the hyperfine tensor and the angle(s) describing the relative orientation of the  $g$  tensor and hyperfine tensor.<sup>12</sup> A comparison of experimental and simulated angle-selected spectra for Act-BLM is shown in the Supporting Information, Figure 1S. A good fit to the overall compendia of angle-selected  $^{19}\text{F}$  ENDOR features from the Act-BLM ( $\text{GGAAGC}^{\text{FTTCC}}_2$ ) complex was provided by a  $^{19}\text{F}$

(11) Hoffman, B. M.; DeRose, V. J.; Doan, P. E.; Gurbel, R. J.; Houseman, A. L. P.; Telsler, J. In *Biological Magnetic Resonance, Vol. 13: EMR of Paramagnetic Molecules*; Berliner, L. J., Reuben, J., Eds.; Plenum: New York, 1993; Vol. 13.

(12) The point dipolar interaction between a nuclear spin  $\mathbf{I}$  and electron spin  $\mathbf{S}$  separated by a distance  $\mathbf{R}$  is  $A_{\text{D}} = \{1/hR^3\}(3(\mu_{\text{S}} \cdot \mathbf{R})(\mu_{\text{I}} \cdot \mathbf{R})/R^2 - \mu_{\text{S}} \cdot \mu_{\text{I}})$ . The nuclear moment is  $\mu_{\text{I}} = g_{\text{n}}\beta_{\text{n}}(I_x + I_y + I_z)$ , and the electron magnetic moment in the  $g$ -tensor principal axis system is  $\mu_{\text{S}} = \beta_{\text{e}}(g_x S_x + g_y S_y + g_z S_z)$ .  $g_{\text{n}}$  is the nuclear  $g$ -value ( $=5.254$  for  $^{19}\text{F}$ ).  $\beta_{\text{e}}$  and  $\beta_{\text{n}}$  are the Bohr magneton and the nuclear magneton, respectively.

hyperfine tensor with components  $A_z, A_y, A_x = 0.48 \pm 0.01, -0.23 \pm 0.01, -0.20 \pm 0.03$  MHz, where the principal hyperfine ( $z$ ) axis defined by the  $\text{Fe}(\text{III})\text{-}^{19}\text{F}$  vector ( $\mathbf{R}$ ) made an angle of  $10^\circ$  in the  $g_{\text{max}}\text{-}g_{\text{min}}$  plane with respect to the  $g_{\text{max}}$  axis. This hyperfine tensor was well explained by dipolar coupling, and the predicted distance from  $^{19}\text{F}$  of 2'-cytidine to  $\text{Fe}(\text{III})$  of Act-BLM was  $7.0 \pm 0.2$  Å. Angle-selected ENDOR (Supporting Information, Figure 2S) also predicted for  $\text{Fe}(\text{III})\text{-BLM}$  a similar  $6.8 \pm 0.2$  Å distance and collinearity of  $\mathbf{R}$  with  $g_{\text{max}}$ . In principle, covalency may alter electron spin density on the iron and alter the estimate of  $\mathbf{R}$ ; however, if the theoretical estimate of 95% spin on the iron<sup>13</sup> is appropriate, the covalent correction to  $\mathbf{R}$  would be small ( $\sim -0.1$  Å). The  $^{31}\text{P}$  couplings observed for complexes of  $\text{d}(\text{GGAAGC}^{\text{FTTCC}})_2$  were the same as those previously measured for  $\text{d}(\text{GGAAGCTTCC})_2$ .<sup>7b</sup> Although it was not possible to observe angle-selected ENDOR of the smaller, 0.13 MHz splitting except near  $g_{\text{max}}$ , such a  $^{19}\text{F}$  coupling was expected (see Supporting Information) from the more distant 2'-cytidine on the complementary oligonucleotide strand.

Our  $\text{Fe}\text{-}2'\text{F}$  distances may be compared to analogous distances from plausibly relevant NMR-derived Co-BLM-oligonucleotide structures. For a  $\text{HOO}\text{-Co}(\text{III})\text{-BLM}$  complex with a 12 base-pair, covalently linked, gapped duplex, the  $\text{Co}\text{-H}2''$  distance was 8.0 Å;<sup>5g</sup> with 6-mer<sup>5c</sup> or 10-mer<sup>5a</sup> duplexes it was 6.1 Å. Our directly determined  $\text{Fe}(\text{III})\text{-}2'\text{F}$  distance was 6.8–7.0 Å. These NMR structures support our assigning the 7.4 Å  $\text{Fe}(\text{III})\text{-}^{31}\text{P}$  distance<sup>7b</sup> to the  $\text{dC}_6$  3'-phosphate in  $\text{d}(\text{GGAAGCTTCC})_2$ . This  $\text{dC}_6$ -3' phosphate is adjacent to the 2'F of the present ENDOR study. The 2'F-Fe-3'P angle of  $27 \pm 5^\circ$  calculated by combining the  $^{31}\text{P}$  hyperfine tensor<sup>7b</sup> with our present  $^{19}\text{F}$  tensor (from either Act-BLM or  $\text{Fe}(\text{III})\text{-BLM}$  complexes) lies within the 17–29° range for the analogous  $\text{H}2''\text{-Co}\text{-}3'\text{P}$  angles of the NMR structures.<sup>5a,c,g</sup> Our  $^{19}\text{F}$  dipolar tensor indicates that the  $\text{Fe}\text{-}2'\text{F}$  direction nearly coincides with  $g_{\text{max}}$ . Combining this directional information with the assumption that the  $\text{Fe}$  and 2'F coordinates approximate those of  $\text{Co}$  and  $\text{H}2''$  coordinates in the Co-BLM-oligonucleotide NMR structure<sup>5g</sup> implies that the  $g_{\text{max}}$  axis tilts at about  $35^\circ$  to the  $\text{Fe}\text{-proximal}\text{-O}$  vector, rather than being collinear with it. (See Supporting Information for the schematic showing  $g$ -tensor,  $\text{Fe}$ ,  $^{31}\text{P}$ ,  $^{19}\text{F}$ , and  $\text{HOO}^-$  geometry.) In summary, the dipolar hyperfine coupling determined between the cytidine-2' $^{19}\text{F}$  and the  $\text{Fe}$  of Act-BLM or of  $\text{Fe}(\text{III})\text{-BLM}$  provides a definitive constraint on the distance between the BLM  $\text{Fe}$  and the 2' substituent of the cytidine sugar where  $\text{H}4'$  abstraction occurs.

**Acknowledgment.** Support was in part by NIH Grant No. GM 35103. Unpublished structural coordinates for ref 5a were kindly provided by Profs. J. Stubbe and A. P. Grollman and Mr. J. Chen.

**Supporting Information Available:** Preparation of  $\text{Fe}(\text{III})\text{-BLM}$  and Act-BLM complexes; information on the weakly hyperfine coupled 2'F; experimental and simulated angle-selected ENDOR spectra from Act-BLM; angle-selected ENDOR spectra vs  $g$  values for  $\text{Fe}(\text{III})\text{-BLM}$ ; and schematic showing orientation of the  $g$ -tensor,  $\text{Fe}^{3+}$ ,  $^{31}\text{P}$ , and  $^{19}\text{F}$  of the cytidine sugar, and NMR-determined  $\text{HOO}^-$  (PDF). This material is available free of charge via the Internet at <http://pubs.acs.org>.

JA016943T

(13) Neese, F.; Zaleski, J. M.; Zaleski, K. L.; Solomon, E. I. *J. Am. Chem. Soc.* **2000**, *122*, 11703–11724.